HURRICANE ISABEL (2003): NEW INSIGHTS INTO THE PHYSICS OF INTENSE STORMS. PART II
Extreme Localized Wind

by Sim D. Aberson, Michael T. Montgomery, Michael Bell, and Michael Black

A dropwindsonde released into a misoscale feature on the inner edge of the eyewall of Hurricane Isabel measured the strongest documented horizontal wind in a tropical cyclone, consistent with the mechanism described in Part I.

Big whirls have little whirls
that feed on their velocity;
and little whirls have lesser whirls,
and so on, to viscosity
—in the molecular sense.

—Lewis Fry Richardson

On 13 September 2003, a dropwindsonde released along the inner edge of the eastern eyewall of Hurricane Isabel measured 107 and 25 m s^{-1} horizontal and vertical winds, respectively, at about 1400 m above sea level. This is the strongest known horizontal wind directly measured in a tropical cyclone (TC),[1] and is in the upper 1% of measurements for the vertical wind (Black et al. 1996). The behavior of the instrument suggests an eyewall misocyclone[2] in a strong convective burst. This particular observation, along with concurrent ob-servations of very fast wind from airborne Doppler radar and other airborne instruments, has important practical implications for emergency management planning, structural wind engineering, and scien-tific interests relating to TC potential intensity and intensity change.

The relatively quiescent environment in which Hurricane Isabel persisted for 3 days (low envi-ronmental shear, no interactions with midlatitude or tropical upper-tropospheric troughs, relatively uniform 27°C sea surface temperature) allowed the TC to remain at or near category-5 status during that period. This environment and the observations taken during this time provide an unprecedented opportunity to gain important insight into eyewall misocyclones and maximum potential intensity.

Persing and Montgomery (2003) found that in high-resolution axisymmetric TC simulations, storm intensity, as defined by the maximum sustained tan-

---

[1] A report of 117 m s^{-1} from a dropwindsonde released in Hurricane Katrina (2005) is unconfirmed due to an apparent loss of raw data.

[2] A misocyclone is defined as a vortex in the horizontal plane, usually within a convective storm, with a width of between 40 m and 4 km. A mesocyclone is a vortex 2–10 km in diameter in a convective storm.

gential wind speed at the top of the boundary layer, greatly exceeds currently understood upper bounds for maximum potential intensity of the steady, axisymmetric vortex (Emanuel 1986, 1988, 1995). They termed this phenomenon "superintensity" and demonstrated that it occurs because of an enhance-
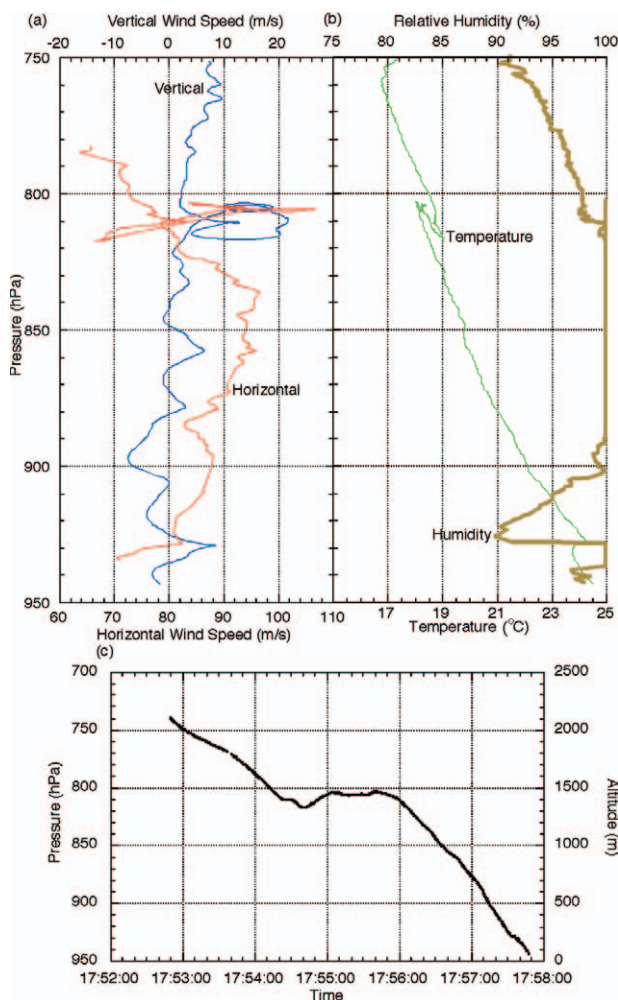

Fig. 1. Data obtained by the dropwindsonde released inside the inner edge of the eyewall of Hurricane Isabel at 1752 UTC 13 Sep 2003: (a) horizontal and vertical wind speeds as a function of pressure, (b) temperature and relative humidity as a function of pressure, and (c) altitude and pressure as a function of time.

ment of entropy at low levels in the hurricane eye. They suggested that the high-entropy air is mixed into the eyewall by mesocyclones at the interface between the eye and the eyewall. The mesocyclones act to mix high moist entropy air from the eye into the eyewall, providing more power to the hurricane engine relative to that obtained from the ocean surface directly underneath and outside of the eyewall. The current study places the small-scale extreme wind observations in Hurricane Isabel ("Extreme wind observations") within the context of this superintensity theory ("Discussion") for the mean vortex structure described in Montgomery et al. (2006, hereafter Part I). Related observations and practical implications from other TCs are also presented.

EXTREME WIND OBSERVATIONS. At 1752 UTC 13 September 2003 a GPS dropwindsonde (Hock and Franklin 1999) was released just inside the eastern edge of the eyewall of Hurricane Isabel just below 750 hPa, or about 2 km above mean sea level. The dropwindsonde encountered a very strong updraft and horizontal wind at the top of a saturated air layer (Fig. 1). The horizontal wind reached 107 m s^{-1}; a nearly 25 m s^{-1} updraft caused the instrument to rise ~200 m and remain suspended for about 90 s before resuming its regular descent. When the descent resumed, the air temperature was about 1 K cooler than that at the same level in the strong updraft, consistent with convective instability. During the time the instrument was suspended, the horizontal wind speed oscillated between ~70 and 100 m s^{-1} at least three times, suggesting a strong rotational wind component on a much smaller scale than the axisymmetric mean circulation, i.e., an eyewall misocyclone.

A dual-airborne Doppler radar analysis was performed from National Oceanic and Atmospheric Administration (NOAA) P-3 tail radar data (Jorgensen et al. 1983) collected from 1749 to 1755 UTC, 3 min before and after the dropwindsonde release. A three-dimensional variational synthesis approach (Gamache et al. 1995) was used with 1.5- and 0.5-km grid spacing in the horizontal and vertical

AFFILIATIONS: ABERSON AND BLACK—NOAA/AOML/Hurricane Research Division, Miami, Florida; MONTGOMERY—Department of Meteorology, Naval Postgraduate School, Monterey, California, and NOAA Hurricane Research Division, Miami, Florida; BELL— Colorado State University, Fort Collins, Colorado and NCAR, Boulder, Colorado
CORRESPONDING AUTHOR: Sim Aberson, NOAA/AOML/ Hurricane Research Division, 4301 Rickenbacker Causeway, Miami, FL 33149

E-mail: sim.aberson@noaa.gov

directions, respectively, and a single-step Leise-scale filter (Leise 1982) was applied to the final wind field. The Doppler synthesis inherently smooths the derived wind both temporally and spatially, particularly vertical velocity. The analyzed reflectivity, wind speed, vorticity, and vertical velocity at 1-km altitude are shown in Fig. 2, strongly supporting the reliability the dropwindsonde measurements. A broad swath of horizontal wind speed exceeding 90 m s⁻¹ is evident in the eyewall; strong radial shear of the horizontal wind with a peak vorticity of 15×10^{-3} s⁻¹ is found on the inner edge of the eyewall near the aircraft track, upwind of a Doppler-derived 5 m s⁻¹ updraft. The dropwindsonde may have been released into this particular feature because it was being advected cyclonically along the inner-edge of the eyewall.

Horizontal and vertical wind profiles directly below the aircraft from the Imaging Wind and Rain Airborne Profiler (IWRAP; Esteban-Fernandez et al. 2005) at the dropwindsonde release time (Fig. 3) shows horizontal and vertical wind speeds approaching 100 and 25 m s⁻¹, respectively. These observations offer independent corroboration of the extreme wind measured by the dropwindsonde and that the feature slopes upwind.

DISCUSSION. The dropwindsonde measured winds in Hurricane Isabel associated with an eyewall misocyclone that are significantly stronger than the suggested "superintense" wind of the mean vortex (Part I). In high-resolution numerical axisymmetric model simulations, very strong, or superintense, wind occurs when high-entropy air is mixed into the eyewall by mesocyclones in the eye at low levels (Persing and Montgomery 2003). This high-entropy air acts as an additional heat source to the eyewall, providing local convective instability (Eastin et al. 2005; Braun 2002). Figure 4 shows the equivalent potential temperature (θ_e) measured by three separate dropwindsondes—the one already discussed; one released in the eyewall 11 km from, and about a minute after, the first; and a third released in the eye by an Air Force Reconnaissance aircraft less than 30 min before the first two. The low-level θ_e in the eye is about 20 K higher than that in the eyewall, representing a
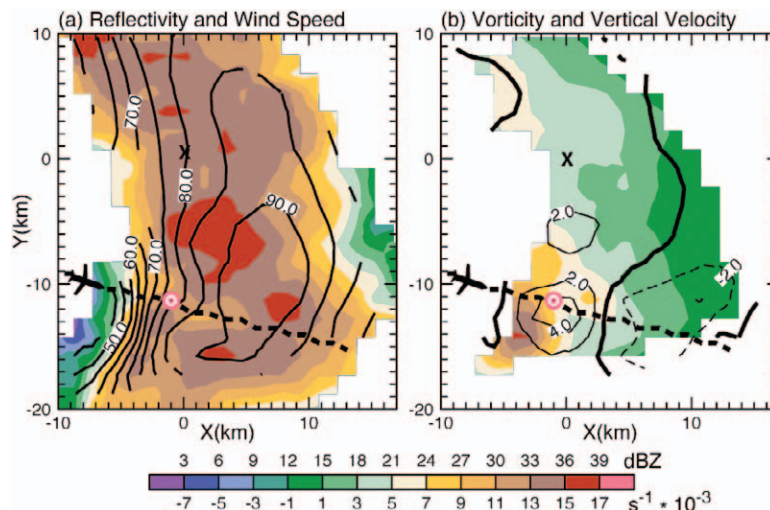

FIG. 2. Dual-airborne Doppler analysis from **NOAA P-3** tail radar at 1-km altitude at 1749–1755 UTC 13 Sep 2003: (a) average reflectivity from fore and aft scans in color (dBZ) and contoured horizontal wind speed (m s⁻¹), and (b) vorticity (×10⁻³ s⁻¹) in color and contoured vertical velocity (m s⁻¹) [upward (thin solid), zero (thick solid), and downward (dashed) motions]. In each panel, the dashed line shows the aircraft flight track during the analysis period; the bullseye indicates the dropwindsonde release location; and the origin (0,0) indicated by an "x" is the location of the record wind speed observation ~2.5 min after the dropwindsonde release.
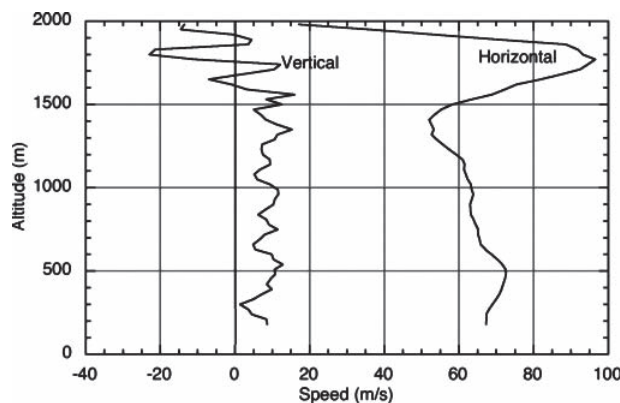

FIG. 3. Horizontal and vertical wind speed profiles obtained by the IWRAP instrument at 1752 UTC 13 Sep 2003 in Hurricane Isabel.

large potential energy source that, if mixed into the eyewall, may cause convective bursts as described above. The θ_e in the feature is about 5 K higher than that in the eyewall itself. Assuming that the second and third observations represent the thermodynamic structure in the eyewall and eye, respectively, the thermodynamic structure of the profile with extreme wind suggests either that there is a mixing of air between the very high entropy eye and the lower entropy eyewall, or that the air sampled originated below the eyewall after it gained entropy from surface
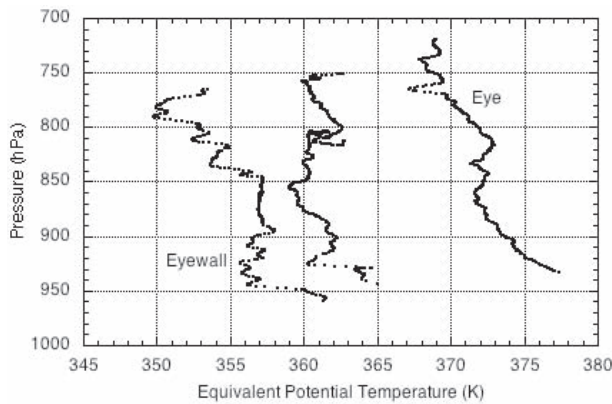
Fig. 4. Equivalent potential temperature profiles obtained by three dropwindsondes—one in the eyewall, one along the interface between the eye and eyewall, and one inside the eye, at approximately the same time on 13 Sep 2003 in Hurricane Isabel. Note that the sea surface slopes upward to lower pressure from the eyewall to the eye.

flux. This instability may spur local, strong convective updrafts and a subsequent acceleration of the horizontal wind by concentrating the high angular momentum of the swirling eyewall flow, similar to that described in Persing and Montgomery (2003), but on a smaller scale.

Figure 5 shows fingers of high reflectivity extending from the eyewall into the eye, and other cellular reflectivity maxima inside the inner edge of the eyewall at about the dropwindsonde release time. These features can be tracked in subsequent radar sweeps and are calculated to be rotating along the inner edge of the eyewall at roughly 70–80 m s^{-1}, coinciding approximately with the mean observed low-level wind speed. The dropwindsonde was released into the feature marked in the figure, and suspended within it during the time of the extreme wind measurement. The filamentary features on the inner edge of the eyewall resemble small-scale Kelvin–Helmholtz instability that feeds off the kinetic energy of the intense cyclonic shear region in the inner edge of the eyewall. Similar vortex tube–like features, aligned in the vertical, also have been observed in the eyewall of Hurricane Erin (Aberson and Halverson 2006). This particular feature is evident in the vertical cross section from a tail radar single sweep (Fig. 5b). It extends nearly to flight level and is inside the main eyewall. The misocyclone is a shallow (altitude <2 km), concentrated core of relatively high reflectivity surrounded by an extremely sharp reflectivity gradient. The vertical and horizontal gradients are extremely large, with the reflectivity decreasing below the threshold detectable by the radar less than 1 km
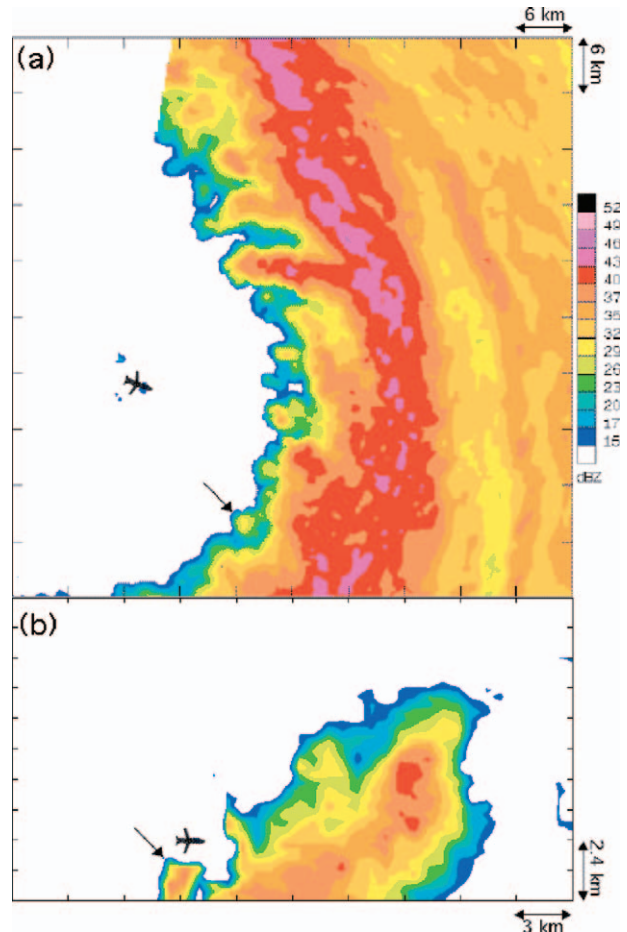

Fig. 5. Radar reflectivity of the eastern eyewall of Hurricane Isabel. (a) Close-up single sweep of the NOAA WP-3D lower-fuselage radar at 1750:35 UTC 13 Sep 2003, showing the filamentary features in the eastern eyewall. The arrow points to the feature the dropwindsonde sampled. (b) A single sweep close-up from the tail radar at 1752:50 UTC the same day showing the vertical structure of the sampled feature and the eyewall. In both panels, the aircraft symbol represents the P-3 location.

from the core. These very high reflectivity gradients are rarely found, except in highly vortical structures (e.g., tornadoes), consistent with the classification of this feature as a misocyclone. The aircraft appears to have flown near the top of the feature, and this is corroborated by the flight-level data (Fig. 6). Notably, the difference between the observation height on a constant pressure surface and its corresponding standard altitude (*D*-value) ceases to increase just before the dropwindsonde was released, with a nearly 45-m maximum deviation from the linear trend. At the same time, the flight-level wind also stopped increasing, then rapidly increased by more than 20 m s^{-1} along with an anticyclonic 20° wind shift.
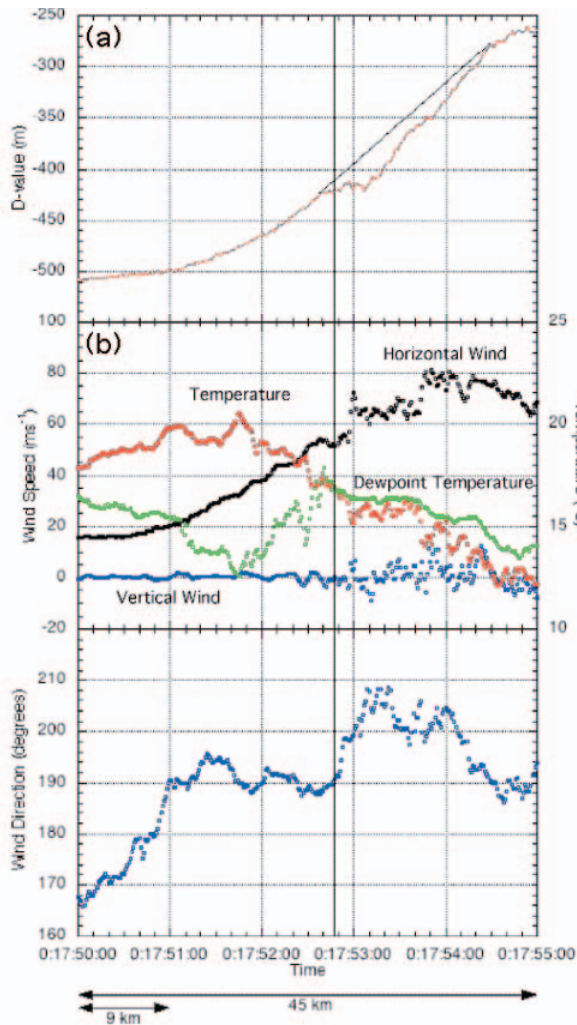
FIG. 6. Flight-level data from the NOAA WP-3D aircraft in the eastern eyewall of Hurricane Isabel between 1750 and 1755 UTC 13 Sep 2003: (a) *D*-value, **(b)** temperature, dewpoint temperature, horizontal wind speed, and vertical wind speed, and **(c)** wind direction. The horizontal line marks the dropwindsonde release time. The WP-3D moves at approximately 9 km min⁻¹, so the entire scale is about 45 km.
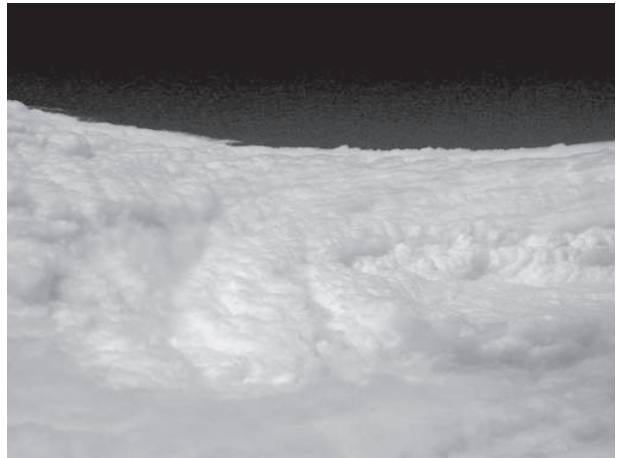

FIG. 7. Digital photograph of the eyewall of Hurricane Isabel taken 12 Sep 2003 from the NOAA WP-3D aircraft while inside the eye. The curved, finger-like feature is seen in the middle of the photograph.

Therefore, though the feature seems to be strongest below, some signature is evident at the flight level as the plane passed over.

Similar features are clearly seen in photographs of the eyewall of Hurricane Isabel on 12 September, and also in other intense tropical cyclones (Bluestein and Marks 1987). Although no suitable photograph of the specific feature described here exists, in the middle of Fig. 7, curved and finger-like features in the eye connecting to the eyewall and sloping radially outward with height are similar in shape and scale to those seen in the radar reflectivity on 13 September. Cellular convective features, also similar in scale to those seen in the radar

reflectivity and the feature into which the dropwindsonde was released, are evident along the inner edge of the eyewall on the right side of the photograph.

RELATED CASES AND IMPLICATIONS.

The above analysis is based on the most comprehensive set of observations of a feature similar to that encountered by the NOAA P-3 aircraft about 450 m above the surface in category-5 Hurricane Hugo on 15 September 1989 (Marks and Black 1990; Black and Marks 1991). The θ_e in the eye of Hugo at that altitude was 380 K (Willoughby 1998), similar to that measured in the eye of Isabel. During the Hugo eyewall penetration, the aircraft encountered very large up- and downdrafts, leading to severe turbulence and damage to the aircraft. In the Hugo case, the vertical motions were (m s⁻¹), respectively, 6 up, 6 down, 9 up, 10 down, 21 up, 8 down, and 12 up, comparable to the vertical motions measured by the IWRAP (Fig. 3) and the dropwindsonde (Fig. 1) in Isabel. A local pressure anomaly of 8 hPa was measured within the Hugo feature, more than twice that observed by the aircraft above the feature in Isabel.

Shortly before landfall, the θ_e in the eye of Hurricane Andrew as measured by dropwindsonde was 383 K higher than that in the Isabel eye sounding. This suggests that similar physical processes may have caused the small-scale features that led to the extreme localized damage as Andrew made landfall in south Florida on 23 August 1992 (Wakimoto and Black 1994). The speculation is that downdrafts allowed locally superintense wind to reach the surface in small-scale streaks. If this is correct, it provides additional confirmation of the increase of the esti-

mated intensity of Hurricane Andrew to category 5 at landfall (Landsea et al. 2004).

The observations presented here document the most extreme wind observed in a hurricane, and similar events are possibly rare. However, the high-reflectivity filaments and cellular features along the inner edge of the eyewall are observed in many strong, mature tropical cyclones. Because radar beam geometry precludes observing the low-level features on all individual radar images, only a subsample of radar observations from airborne or ground-based systems would indicate the presence of these features. The similarity between the Isabel misocyclone and features encountered in Hurricanes Hugo and Andrew that led to catastrophic impacts suggests that they may occur with regularity, though their frequency is unknown. Such small-scale features, though heretofore difficult to observe directly, merit further study.

REFERENCES

Aberson, S. D., and J. B. Halverson, 2006: Kelvin-Helmholtz billows in the eyewall of Hurricane Erin. *Mon. Wea. Rev.,* **134,** 1036–1038.

Black, M. L., R. W. Burpee, and F. D. Marks, 1996: Vertical motion characteristics of tropical cyclones determined with airborne Doppler radial velocities. *J. Atmos. Sci.,* **53,** 1887–1909.

Black, P. G., and F. D. Marks, 1991: The structure of an eyewall meso-vortex in Hurricane Hugo (1989). Preprints, *19th Conf. on Hurricanes and Tropical Meteorology,* Miami, FL, Amer. Meteor. Soc., 579–582.

Bluestein, H. W., and F. D. Marks, 1987: On the structure of the eye-wall of Hurricane Diana (1984): Comparison of radar and visual characteristics. *Mon. Wea. Rev.,* **115,** 2542–2552.

Braun, S. A., 2002: A cloud-resolving simulation of Hurricane Bob (1991): Storm structure and eyewall buoyancy. *Mon. Wea. Rev.,* **130,** 1573–1592.

Eastin, M. D., W. M. Gray, and P. G. Black, 2005: Buoyancy of convective vertical motions in the inner core of hurricanes. Part II: Case studies. *Mon. Wea. Rev.,* **133,** 209–227.

Emanuel, K. A., 1986: An air-sea interaction theory for tropical cyclones. Part I: Steady-state maintenance. *J. Atmos. Sci.,* **43,** 585–605.

——, 1988: The maximum intensity of hurricanes. *J. Atmos. Sci.,* **45,** 1143–1155.

——, 1995: Sensitivity of tropical cyclones to surface exchange coefficients and a revised steady-state model incorporating eye dynamics. *J. Atmos. Sci.,* **52,** 3969–3976.

Esteban-Fernandez, D., and Coauthors, 2005: IWRAP: The Imaging Wind and Rain Airborne Profiler for remote sensing of the ocean and the atmosphere boundary layer within tropical cyclones. *IEEE Trans. Geosci. Remote Sens.,* **43,** 1775–1787.

Gamache, J. F., F. D. Marks, and F. Roux, 1995: Comparison of three airborne Doppler sampling techniques with airborne in situ wind observations in Hurricane Gustav (1990). *J. Atmos. Oceanic Technol.,* **12,** 171–182.

Hock, T. F., and J. L. Franklin, 1999: The NCAR GPS dropwindsonde. *Bull. Amer. Meteor. Soc.,* **80,** 407–420.

Jorgensen, D. P., P. H. Hildebrand, and C. L. Frush, 1983: Feasibility test of an airborne pulse-Doppler meteorological radar. *J. Climate Appl. Meteor.,* **22,** 744–757.

Landsea, C. W., and Coauthors, 2004: A reanalysis of Hurricane Andrew's intensity. *Bull. Amer. Meteor. Soc.,* **85,** 1499–1712.

Leise, J. A., 1982: A multidimensional scale-telescoped filter and data extension package. NOAA Tech. Memo ERL WPL-82, 19 pp.

Marks, F. D., and P. G. Black, 1990: Close encounter with an intense mesoscale vortex within Hurricane Hugo (September 15, 1989). Preprints, *Fourth Conf. on Mesoscale Processes,* Boulder, CO, Amer. Meteor. Soc., 114–115.

Montgomery, M. T., M. Bell, S. D. Aberson, and M. Black, 2006: Hurricane Isabelle (2003): New insights into the physics of intense storms. Part I: Mean vortex structure and maximum intensity estimate. *Bull. Amer. Meteor. Soc.,* **87,** 1335–1347.

Persing, J., and M. T. Montgomery, 2003: Hurricane superintensity. *J. Atmos. Sci.,* **60,** 2349–2371.

Wakimoto, R. M., and P. G. Black, 1994: Damage survey of Hurricane Andrew and its relationship to the eyewall. *Bull. Amer. Meteor. Soc.,* **75,** 189–200.

Willoughby, H. E., 1998: Tropical cyclone eye thermodynamics. *Mon. Wea. Rev.,* **126,** 3053–3067.